Panamerican Mathematical Journal
ISSN: 1064-9735
Vol 35 No. 2s (2025)

Quantitative Analysis of Natural Calamities for Disaster Management through Machine Learning Techniques Using Satellite Data

Nita Nimbarte[1], Megha Chakole[1], Sanjay Balamwar[2], Ajinkya Nilawar[3], Suresh Kurumbanshi[4], Rajendra Rewatkar[5]

[1]Department of Electronics & Telecommunication Engineering, Yeshwantrao Chavan College of Engineering, Nagpur, India. nitangp@gmail.com, mdorle@gmail.com

[2]Maharashtra Remote Sensing and Applications Centre (MRSAC), VNIT Campus, Nagpur, India. Sanjay.balamwar@mrsac.maharashtra.gov.in

[3]Electronics and Communications Engineering, Ramdeobaba University,Nagpur. aa.nilawar@gmail.com

[4]Mukesh Patel School of Technology, Management and Engineering,SVKM's NMIMS, Shirpur Campus. sureshkurumbanshi@gmail.com

[5]Biomedical Engineering Department, Faculty of Engineering and Technology, Datta Meghe Institute of Higher Education and Research ,Sawangi (Meghe),Wardha.rajendrar.feat@dmiher.edu.in

Article History:

Received: *16-09-2024*

Revised: *03-11-2024*

Accepted: *11-11-2024*

Abstract:

Geographic information and Remote sensing systems have been used in recent years by disaster platforms for calamity warning and preparedness for earthquakes, landslides, and floods to aid in the assessment and management of catastrophic risk. In the realm of technology, it has also received a lot of attention. It would not be possible to use sensory data without the appropriate technology for organizing enormous amounts of data and obtaining information from numerous sources, such as maps or measurement channels. This study uses machine learning techniques to locate and evaluate locations damaged by landslides, earthquakes, floods, avalanches, and wildfires. After applying filters to improve the quality of the images, the images are classed using both supervised and unsupervised methods after being segmented using a thresholding technique. To analyze devastation, images from before and after disasters are collected from MRSAC Nagpur and processed with Python-based tools, ArcGIS, ERDAS, and QGIS.

Keywords: Natural Calamite, Satellite Data, Disaster, Wildfire, Earthquake, Avalanche, Flood, Landslide

Introduction

All throughout the world, disasters devastate people and property in different ways. The increasing pressure of a growing population on the planet's resources has made humans and their infrastructure more vulnerable to long-standing environmental risks. Today's advanced technology must be used to investigate frequently occurring events such as earthquakes, floods, landslides, and forest fires in order to develop effective preventive measures. Disaster prevention can be aided by improved future scenario projections, the identification of catastrophe-prone areas, the placement of safety precautions and other routes, and other uses of space technology. Following a disaster, satellite data is gathered to assist with damage claims and disaster recovery [1-2].

M. M. A. Syeed et al. offer Binary Logistic Regression, K-Nearest Neighbor (KNN), Support Vector Classifier (SVC), and Decision Tree Classifier [3]. A comparative study was carried out to identify the model that provides the highest level of accuracy. After reviewing multiple articles, T. Sharma et al. [4] discovered that while SVM and Regression are good algorithms, Random Forest and Neural Networks outperform the others. Other algorithms include Bayesian networks, Random Forest approaches, and neural networks. Data about precipitation for Indian states can be found on a number of websites and other sources. Three states were the subject of this evaluation report: Kerala, Bihar, and Uttar Pradesh. MODIS pictures with a 250 m resolution were used, according to an analysis by B. Li et al. [5], to track the region that was flooded and the dynamic changes that took place in the flooding area between 2000 and 2010. According to the data, 2010 saw more area inundated by Poyang Lake than any previous year. The inundated area of Poyang Lake increased between 2000 and 2010, while the east and southwest Dongting Lakes showed a discernible declining trend. Karamat Ali et al.'s [6] demonstration of the different flood risk assessment criteria. The steps in an assessment are describing the location, estimating the level of intensity and danger, and evaluating vulnerability. Additionally, developments in hydraulic modeling technology, geographic information systems (GIS), and remote sensing were reported.

Machine learning approach for early prediction of wildfire detection system was described by S. N. Ghate et al. [7]. The machine learning techniques Random Forest, Logistic Regression, and kNN are employed for analysis utilizing various features such as temperature, pressure, and vegetation. A Convolutional Neural Network (CNN) based image identification system was proposed by M. Rahul et al. [8]. Convolutional layers were added to the refined Resnet50 architecture in order to use the Relu activation function. The algorithm yields an accuracy of 89.57% on test data and 92.27% on the training set of forest fire data. The time scale basis concept is used in the proposed method to detect wildfire areas. Otsu method was modified and utilized to segment the input images. For current data prediction, a Deep Learning and Long Short Term Memory (LSTM) based method is employed [9].

Machine learning approach for early prediction of wildfire detection system was described by S. N. Ghate et al. [7]. arbitrary forest Amirhosein Mosavi et al. [10] employed alternating decision trees (ADT), logistic regression (LR), logistic model trees (LMT), functional trees (FT), and random subspaces (RS) to create a machine learning model for avalanche detection. The analysis is performed using the ROC curve, and the findings are shown as follows: Kappa = 0.782, Sensitivity = 94.1%, Specificity = 92.4%, Accuracy = 93.3%. Three parameters were examined by Bahram Choubin et al. [11]: topographical features, meteorological conditions, and avalanche occurrence locations. Machine learning approaches based on support vector machines (SVM) and multivariate discriminant analysis (MDA) are proposed. For avalanche area analysis, both methods performed superbly, with an area under the curve of more than 90%. SVM technique for high-dimensional data was reported by the author. For avalanche forecasting testing, data was gathered from the Lochaber, Scotland, UK area. When compared to the Nearest-Neighbor (NN) approach, it produces better results [12].

Long-short-term memory (LSTM) and artificial neural network (ANN) based models for earthquake detection and forecasting systems were proposed by B. Bhargava and S. Pasari [13]. With minor to medium-sized earthquakes, both models produce results that are satisfactory. A machine learning-based strategy was developed by B. Arunadevi et al. [14]. Measurement and recording device for earthquake data also in use. Geographic data mining techniques and decision trees were created in the machine learning approach. An algorithm was created by X. Wang et al. [15] utilizing Excel machine learning techniques, random forest, and LSTM neural networks. The random forest method outperforms the LSTM method for classifying major earthquake occurrences and magnitude identification in large-scale databases. Essam Ghamryet al. [16] gave five case studies for earthquake analysis. Magnetic data is analyzed using the Discrete Cosine Transform (DCT) and Fast Fourier Transform (FFT) techniques. Swarm satellites collected magnetic data in the upper side ionosphere in conjunction with MODIS and MERRA-2. Convolutional neural networks are used to develop a multilevel feature augmentation network for landslide analysis. Three models are described [17] in order to detect changes in landslide areas.

Various techniques, including Efficient Det, YOLOV5, SSD, Faster RCNN, and the enhanced YOLOV5, were presented by W. Zhang et al. [18] for landslide detection. With 57 seconds of training time per epoch, the SSD algorithm achieved a reported accuracy of 97.86%. A pixel-based segmentation method for landslide detection using Mask R-CNN is provided. There are three processes involved in this process: increasing the size of the training dataset, using a small sample with fine tuning, and calculating the F1 measure, recall, and precision [19]. Numerous research articles have offered machine learning and deep learning methodologies, as well as difficulties and solutions for disaster analysis [20]. This article covered a number of disaster mechanisms. Preprocessed input data had enhanced quality and was characterized more precisely. For categorization, supervised machine learning techniques like the maximum likelihood method are employed.

I. Materials and Methods

The USGS Earth Explorer and MRSAC Nagpur Datasets are the sources of the sample input images. Disaster prevention uses these unprocessed satellite image taken both before and after events. Disaster analysis takes into account a variety of events, including avalanches, landslides, earthquakes, floods, and forest fires.

A. *ERDAS IMAGINE Tool Approach*

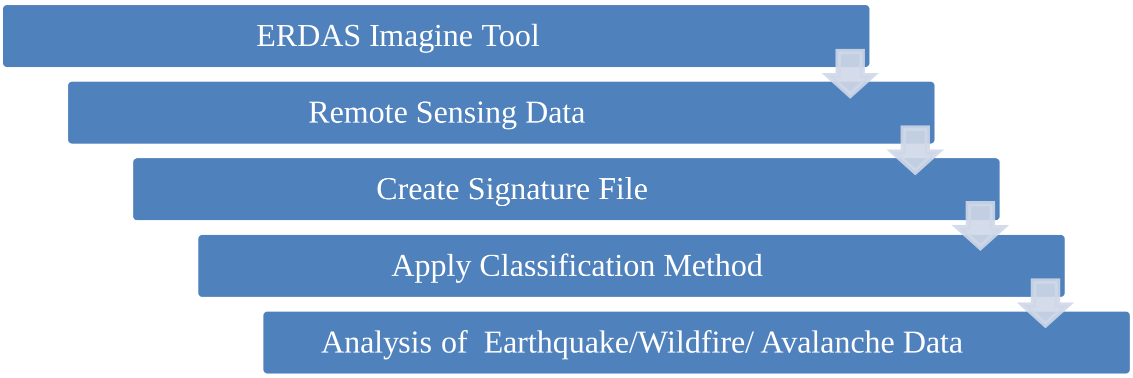

Figure 1. Steps for Disaster analysis using ERDAS Imagine Tool.

Panamerican Mathematical Journal
ISSN: 1064-9735
Vol 35 No. 2s (2025)

Figure 1 illustrates the steps for avalanche, wildfire and earthquake image analysis using ERDAS Imagine tool. ERDAS imagine provides greater raster and vector integration helping to minimize workflow performance. Using the Raster tab in the ERDAS IMAGINE program, choose the proper classification method. Using this geometric tool, construct signature files for each class in the supervised classification technique. Next, signature files are employed to further categorize the objects. To classify items using an unsupervised classification approach, a number of classes must be entered. Further classification process is carried out automatically.

1) ***Wildfire Analysis***

Both supervised and unsupervised classification techniques are applied in the assessment of wildfires. As seen in Figure 2, signature files are generated in ERDAS for various classes. Segmentation is another usage for this signature file. Most Likelihood under supervision for classification, the classification approach is applied. Similarly, unsupervised classification was accomplished using the ISO cluster-based classification method. Images obtained before and after the fire are used to examine the charred region, as shown in Figure 3. Following segmentation, the burned area is represented by the color pink radish.

Class #	>	Signature Name	Color	Red	Green	Blue	Value	Order
1		Class 1		0.651	0.651	0.651	1	1
2		Class 2		0.650	0.650	0.650	2	2
3		Class 3		0.571	0.571	0.571	3	3
4		Class 4		0.276	0.276	0.276	4	4
5		Class 5		0.299	0.299	0.299	5	5
6		Class 6		0.385	0.385	0.385	6	6
7	▶	Class 7		0.558	0.558	0.558	7	7

Figure 2. Classes shown Signature Editor File for Segmentation

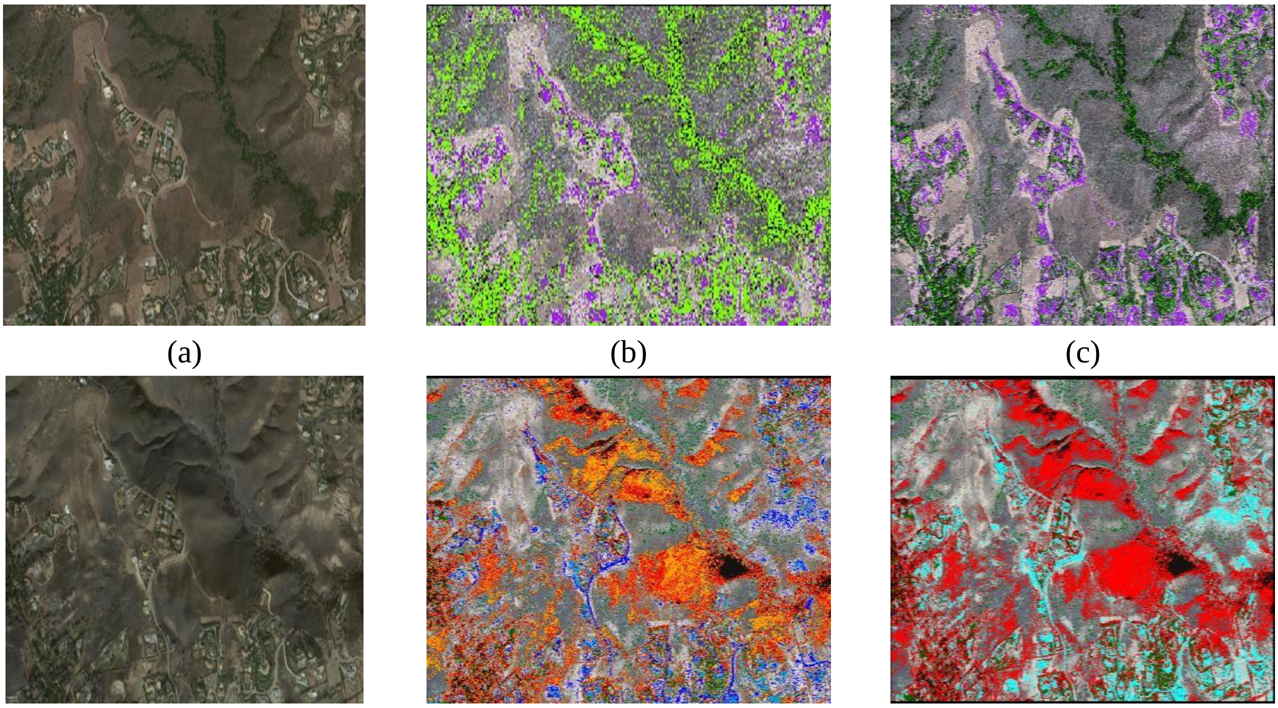

(a) (b) (c)

(d) (e) (f)

Figure 3. Wildfire Analysis: (a) Location: Malibu, California Year: November 2017 (Before Wildfire), (b) Result of Supervised Method, (c) Result of Unsupervised Method, (d) Location:

Malibu, California Year: August 2018 (After Wildfire), (e) Result of Supervised Method, (f) Result of Unsupervised Method.

2) ***Earthquakes Analysis***

ERDAS is one such package has been adopted in recent regional projects for earthquake hazard assessment in Indonesia, Nepal and Japan etc. For doing earthquake assessment, first we have to get a shape image of area of interest. After getting the shape image of required location, convert the vector image into a raster. By converting a vector image into a raster extract all the information stored in the file. Points, lines, and polygons make up the data in this format. Vector data is made up of discrete points that are recorded as coordinate pairs and indicate a physical position in the world. A shapefile is a simple, non-topological format for storing the geometric location and attribute information of geographic features.

For performing supervised classification, create training samples by selecting pixels of same properties and classes will be formed. Supervised classification is where user decides what class categories user wants to assign pixels or segments. These class categories are referred to as specific classification schema. After the classification is complete, go through the resulting classified dataset and reassign any classes or class polygons to the proper class based on defined schema. Figure 4 is a high-resolution satellite image of location Palu, Indonesia used for Earthquake analysis.

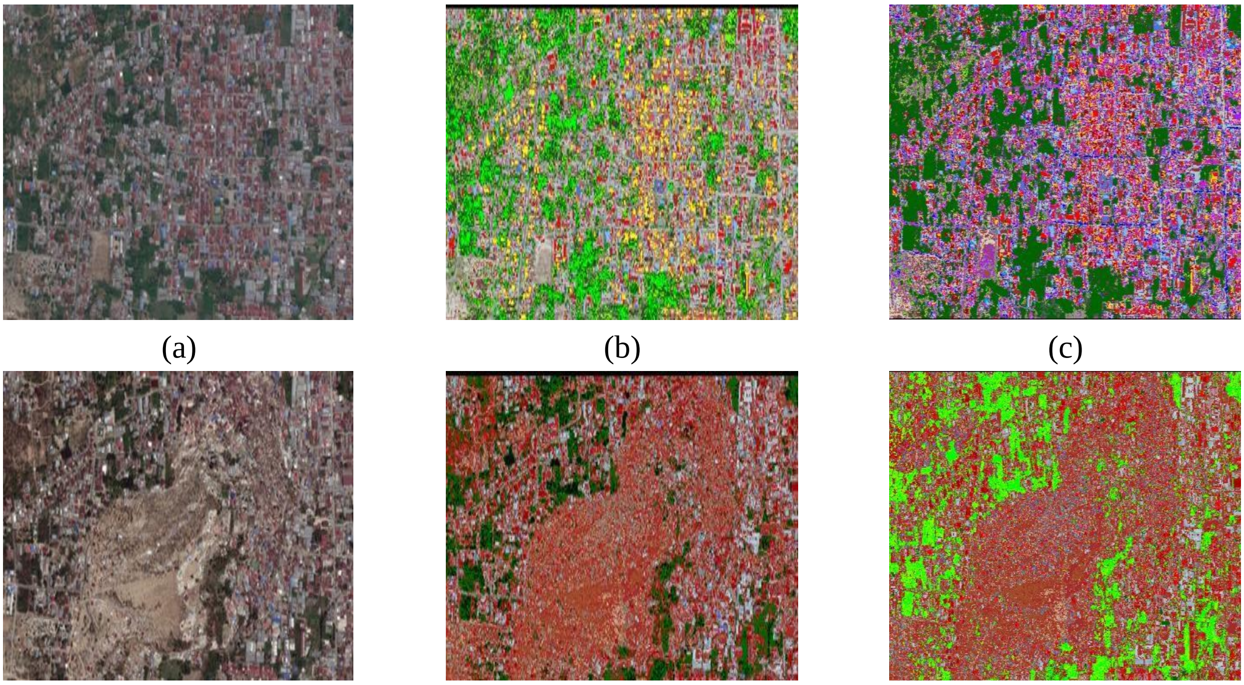

(a) (b) (c)

(d) (e) (f)

Figure 4. Earthquake Analysis: (a) Location Palu, Indonesia Year: August 2018 (Before Earthquake), (b) Result of Supervised Method, (c) Result of Unsupervised Method, (d) Location Palu, Indonesia Year: August 2018 (After Earthquake), (e) Result of Supervised Method, (f) Result of Unsupervised Method.

3) *Avalanche Assessment*

The avalanche evaluation was conducted using the ERDAS technology. To classify the damage region, input images underwent both supervised and unsupervised classification, as illustrated in Figure 5. Several classes that are used to further classify items are defined in the signature editor file. Images of avalanches taken before and after a disaster are compared, and any changes are noted for further examination.

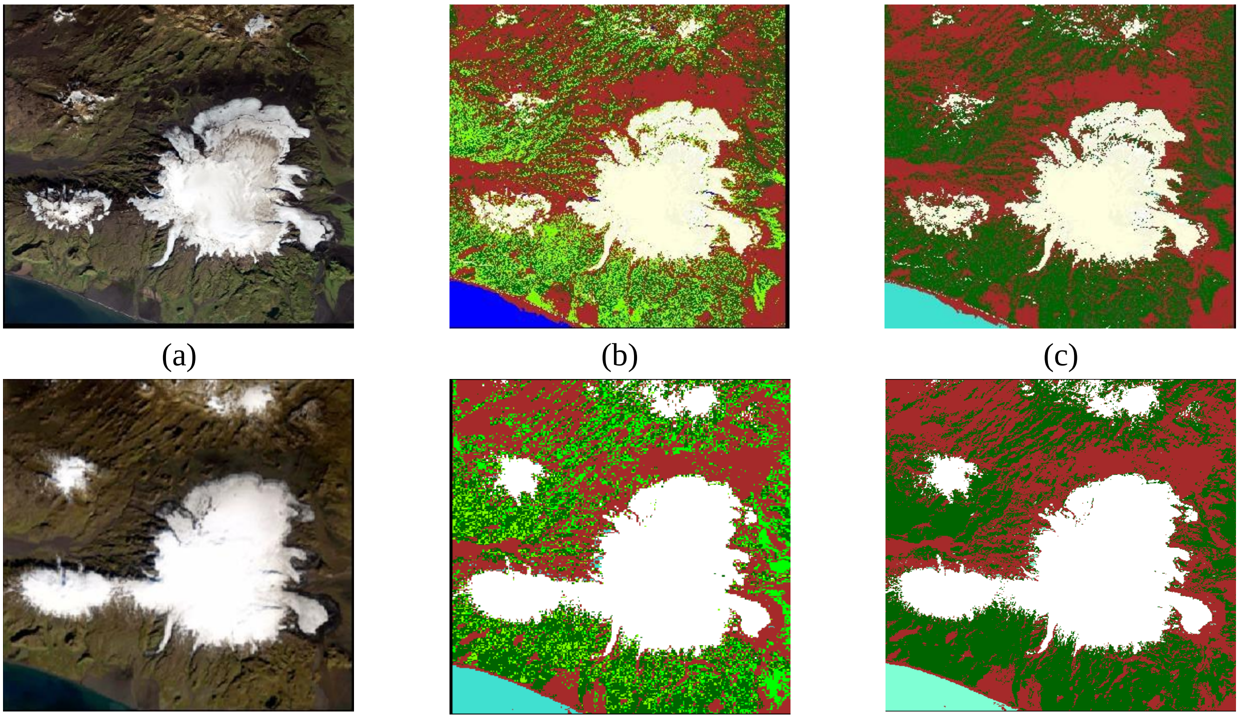

(a) (b) (c)

(d) (e) (f)

Figure 5. Avalanche Analysis: (a) Iceland Year: 24 June 2019 (Before Avalanche), (b) Result of Supervised Method, (c) Result of Unsupervised Method., (d) Iceland Year: 21 July 2019 (After Avalanche), (e) Result of Supervised Method, (f) Result of Unsupervised Method.

B. *ArcGIS Tool Approach*

Figure 6 represented the flood area analysis steps using ArcGIS tool. Make a Digital Elevation Model (DEM) in the ArcGIS simulation tool first. 3D computer graphics, such as mountains, sea depths, and flat terrain, are present in input images that are converted into DEM images. Make shape files with polygons for various characteristics, such as land, sea, etc. Use the ArcScene option to visualize flood modeling more effectively. For additional study, make a 3D animation and alter the color of various objects.

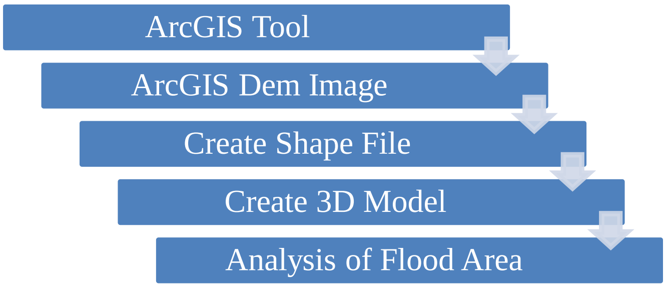

Figure 6. Steps for Disaster analysis using ArcGIS Tool.

1) *Flood Risk Analysis*

Obtaining a Digital Elevation Model (DEM) image of the area of interest, as seen in Figure 7(a), is the first step in doing a flood risk analysis. Next, the DEM image must be converted into a raster format in order to extract all of the information held inside and create a shape file. The shape file contains geographic elements including attribute information and the location of the area of interest (AOI). The shapefile-created 3D model of AOI is shown in Figure 7(b). Determine which locations are susceptible to flooding due to variations in land elevation. It can pinpoint areas with a high risk of flooding, enabling decision-makers to take the appropriate action to minimize damages.

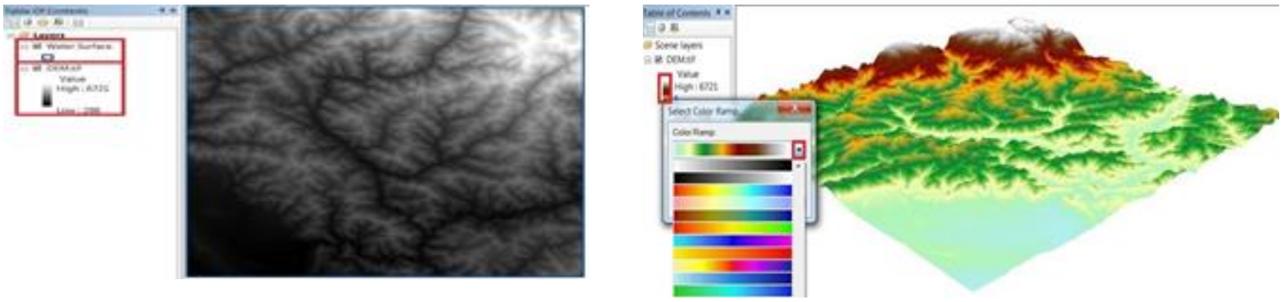

(a) (b)

Figure 7. Flood Analysis: (a) Location: Zaire River, Congo Source: USGS Earth Explorer, (b) Simulation of 3D Model

C. *Python Based Approach*

Figure 8 described python based algorithm for landslide assessment. In the Python-based method, input images are treated beforehand to improve the image quality. Using the thresholding approach, images can be segmented. Segmented image represents objects in different colors, then through pixel values analysis is carried out.

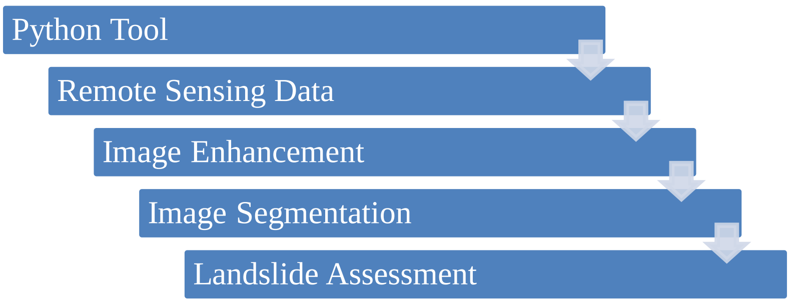

Figure 8. Steps for Disaster analysis using Python Tool.

1) *Landslide Evaluation*

With the aid of Google Earth Pro Software, landset-8, before and after landslide images from the USA, Oso, June 2018 and June 2019 areas were gathered from the MRSAC Nagpur for landslide study. These serve as RGB input images for an algorithm based on Python that analyzes the input data. RGB images were transformed to HSV (Hue Saturation Value) format during the preprocessing stage. Following that, the image was segmented using the thresholding technique, producing the binary image representation seen in Figure 9.

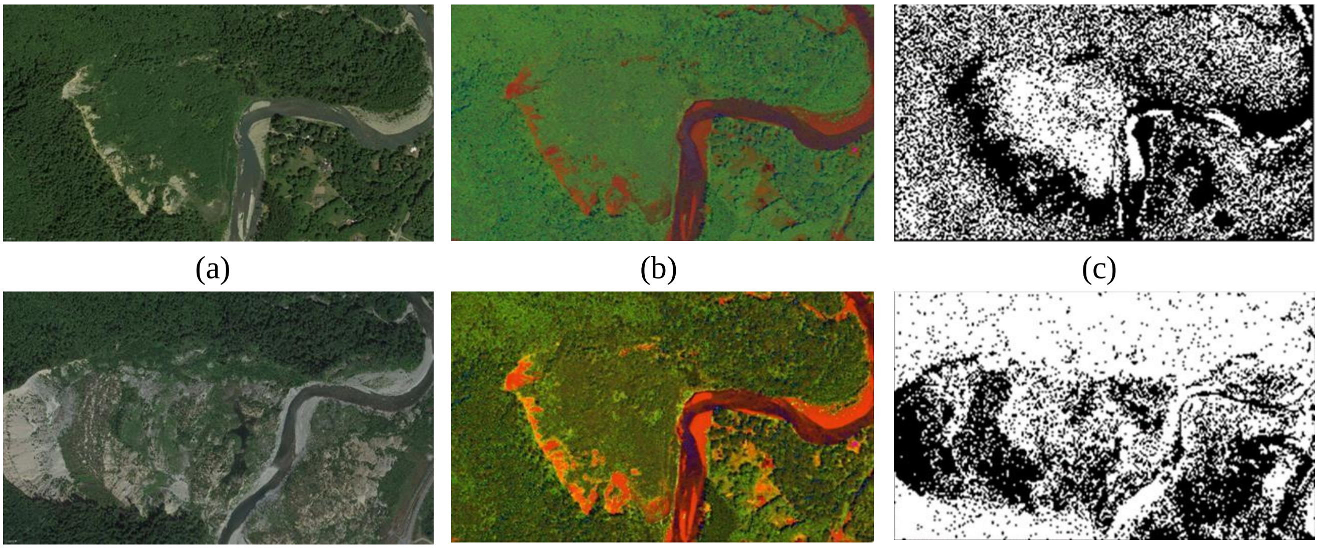

Figure 9. Landslide Analysis OSO, USA: (a) Year: June 2018 (Before Landslide) , (b) RGB to HSV Image Conversion, (c) Thresholded Image, (d) Year: June 2019 (After Landslide), (e) RGB to HSV Image Conversion, (f) Thresholded Image.

II. RESULTS AND DISCUSSION

The outcomes for both supervised and unsupervised classification techniques are shown in Figure 3. For images of wildfires, supervised algorithms get better results. The parameters of the vegetation, land, and burn land area before and after wildfire are shown in Table 1. There are 4892135 pixels in the green land class and 7902518 pixels in the land class overall. The total pixel value for burned land is 0. This image's total pixel value is 12794653. After wildfire, pixels count for vegetation reduced to 2556423. Similarly, pixels count for land reduced to 5060644. Burned land pixels count increases from 0 to 5177586. Figure 10 illustrates how wildfires reduce the overall value of land pixels and green land pixels. The purpose of this analysis is to evaluate the damage that a wildfire has caused.

TABLE I. BEFORE AND AFTER WILDFIRE AREA ANALYSIS

Classification	Pixels Count Before Wildfire	Pixels Count After Wildfire
Vegetation	4892135	2556423
land	7902518	5060644
Burn land	0	5177586
Total	12794653	12794653

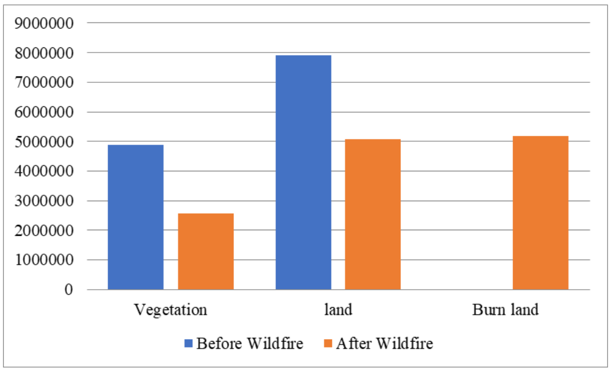

Figure 10. Wildfire Analysis through Graphical Representation.

The parameters for the supervised categorization of the earthquake data before and after are displayed in Tables 2 and 3. Three classes exist: land area, water, and vegetation. For both analysis, there are 13046400 pixels in total. There are 2863870 pixels in the vegetation, or 3282333 pixels. 418463 pixels more vegetation increased during the earthquake. After disaster for Land, 6485251 pixels out of 3802019 pixels are evaluated. Land 6103232 pixels grew in tragedy in earthquake greater. Pixel count 3279816 of which 6380511 are for houses. Pixels in the earthquake house dropped to 3100695. Furthermore, a graphical depiction allows us to observe the difference in pixels as shown in figure 11. In the ERDAS IMAGINE software, the overall accuracy of supervised classification is 98.03% after an earthquake and 96.95% before one.

TABLE II. BEFORE EARTHQUAKE AREA ANALYSIS

Sr.No.	Classification	Pixels Count	Square kilometre	Accuracy
1	Vegetation	2863870	22.71	96.95%
2	land	3802019	24.54	
3	House	6380511	52.73	
Total pixels		13046400	99.98	

TABLE III. AFTER EARTHQUAKE AREA ANALYSIS

Sr.No.	Classification	Pixels Count	Square kilometre	Accuracy
1	Vegetation	3282333	25.15	98.03%
2	land	6485251	49.70	
3	House	3279816	28.58	
Total pixels		13046400	103.43	

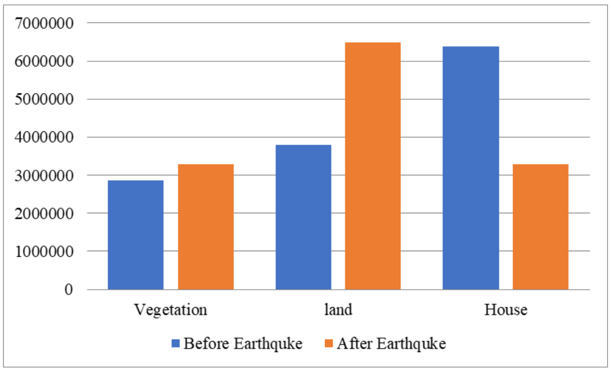

Figure 11. Earthquke Analysis through Graphical Representation.

Results for supervised and unsupervised classification techniques are shown in Figure 5. The resulting image from supervised classification has more details. The parameters of the snow, land, and water areas prior to an avalanche are shown in Table 4. There are 20156 pixels in the snow land class overall, or around 15.85 square kilometers. There are 98560 pixels in the land class overall, or around 77.54 square kilometers. The entire pixel value for water is 8454, covering an area of about 6.6 square kilometers. This image has a total pixel value of 127170 and an accuracy rating of 96.78%

Similarly, the parameters of the snow, land, and water area following an avalanche are shown in Table 5. There are 40412 pixels overall in the snow land class, which equates to an area of about 31.79 square kilometers. There are 78300 pixels in total for the land class, or around 61.6 square kilometers. Water has a total pixel value of 8460, which covers an area of about 6.6 square kilometers. This image's total pixel value is 127172, and its accuracy rating is 97.69%. Figure 10 illustrates how avalanche causes a decrease in the overall land area pixel value. The process of change detection involves comparing avalanche images taken before and after.

TABLE IV. BEFORE AVALANCHE ACCURACY ASSESSMENT

Sr. No.	Classification	Pixels Count	Square kilometre	Accuracy
1	Snow	20156	15.85	**96.78%**
2	Land	98560	77.54	
3	Water	8454	6.6	
	Total pixels	127170	99.99	

TABLE V. AFTER AVALANCHE ACCURACY ASSESSMENT

Sr. No.	Classification	Pixels Count	Square kilometre	Accuracy
1	Snow	40412	31.79	**97.69%**
2	Land	78300	61.6	
3	Water	8460	6.6	
	Total pixels	127172	99.99	

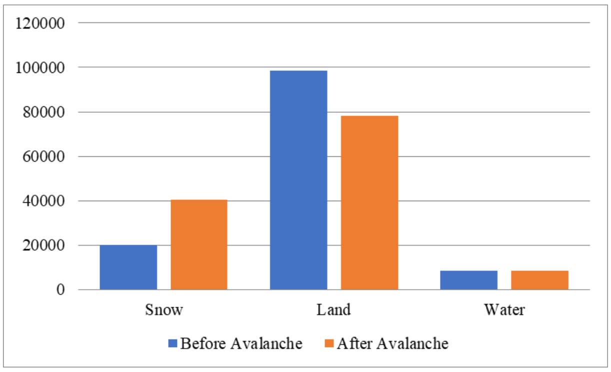

Figure 12. Analysis of Iceland Avalanche Disaster

The 3D model of the Zaire River, Congo location is displayed in Figure 7. The image covers 150.25 square kilometers in total. The area below height level 330 will be totally buried under water if we raise the water level by that amount. The lowest elevation value is 310, and the highest elevation value is 335. 61.84 square kilometers will be completely submerged under water, while 88.41 square kilometers above elevation 310 will be protected from flooding, as depicted in Figure 13. The region below elevation level 330 will be totally buried under water if we raise the water level to that level. The entire region that will be flooded is 77.30 square kilometers, whereas the 72.95 square kilometers that are above elevation level 330 will not be impacted by flooding. The region below elevation level 335 will be totally buried under water if we raise the water level to that level. A total of 92.76 square kilometers will be flooded, whereas 57.49 square kilometers above elevation 398 will not experience any flooding-related damages.

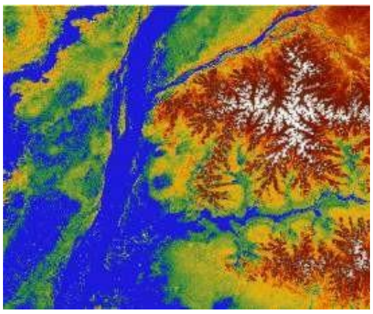

Elevation: 310 and Area: 61.84 sq km

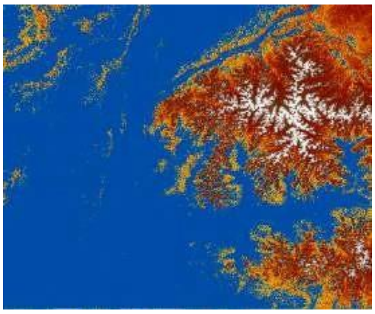

Elevation: 330 and Area: 77.30 sq km

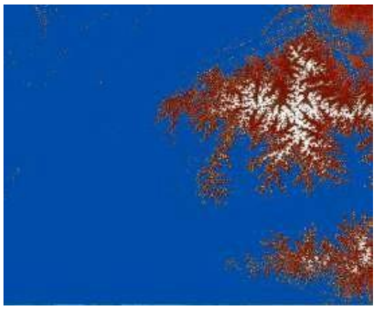

Elevation: 335 Area: 92.76 sq km

Figure 13. Water Area Covered at Different Elevation

In the US, landslides happen in states like Washington and Oregon. The coastal and mountainous regions are the main areas where landslides occur and have the potential to occur. Washington therefore gathered the input data images of Oso USA from June 2018 and June 2019, respectively, before the landslide (Figure 9(a)) and after the landslide (Figure 9(d)). An RGB image was transformed to an HSV color space in order to detect changes in deforestation. Another kind of color space is called an HSV, where the letters H, S, and V stand for hue, saturation, and value, respectively. The vegetation area is shown by the color green in Figures 9(b) and 9(e) throughout a certain time period. The binary form of the input image, referred to as the mask image, is shown in Figures 9(c) and 9(f). When a monochromatic image is employed as a mask, the white area appears 100% transparent, revealing the original image's selected information. It produces a black-and-white image with undesirable areas colored black and white in place of the intended greens. Figure 14 illustrates the final image obtained by combining the original and binary images. Following the landslide disaster, there was a 50.34% loss of vegetation.

(a) (b)

Figure 14. Vegetation Analysis, a) Before Landslide Year: June 2018 , b) After landslide Year: June 2019

III. CONCLUSION

This study covered a number of natural disaster mitigation strategies that can be applied going forward to focus on emergency scenarios. Data from remote sensing is utilized in disaster condition predictions, planning, and management. In order to develop workable preventive measures, it is essential to look into the frequency of earthquakes, floods, landslides, avalanches, and forest fires using today's state-of-the-art technologies. This research article offers a plethora of useful pre- and post-disaster analysis examples. Technique for identifying and classifying the area of interest is provided, utilizing Python, ERDAS, and ArcGIS platform.

ACKNOWLEDGMENT

The Maharashtra Remote Sensing Applications & Centre, Nagpur, is collaborating on the project. We are grateful to them for their knowledge and experience, which were extremely helpful in the creation of the algorithm and its effective application.

References

[1] S. Sreelakshmi and S. S. Vinod Chandra, "Machine Learning for Disaster Management: Insights from past research and future implications," 2022 International Conference on Computing, Communication, Security and Intelligent Systems (IC3SIS), Kochi, India, 2022, pp. 1-7, doi: 10.1109/IC3SIS54991.2022.9885494.

[2] G. Murariu et al., "Disaster management system," 2019 6th International Symposium on Electrical and Electronics Engineering (ISEEE), Galati, Romania, 2019, pp. 1-6, doi: 10.1109/ISEEE48094.2019.9136150.

[3] M. M. A. Syeed, M. Farzana, I. Namir, I. Ishrar, M. H. Nushra and T. Rahman, "Flood Prediction Using Machine Learning Models," 2022 International Congress on Human-Computer Interaction, Optimization and Robotic Applications (HORA), Ankara, Turkey, 2022, pp. 1-6, doi: 10.1109/HORA55278.2022.9800023.

[4] T. Sharma, A. Pal, A. Kaushik, A. Yadav and A. Chitragupta, "A Survey on Flood Prediction analysis based on ML Algorithm using Data Science Methodology," 2022 IEEE Delhi Section Conference (DELCON), New Delhi, India, 2022, pp. 1-8, doi: 10.1109/DELCON54057.2022.9753396.

[5] B. Li, Q. Yan and L. Zhang, "Flood monitoring and analysis over the middle reaches of Yangtze River basin using MODIS time-series imagery," 2011 IEEE International Geoscience and Remote Sensing Symposium, Vancouver, BC, Canada, 2011, pp. 807-810, doi: 10.1109/IGARSS.2011.6049253.

[6] Karamat Ali, Roshan M. Bajracharya and Hriday Lal. Koirala, “A Review of Flood Risk Assessment”, International Journal of Environment, Agriculture and Biotechnology (IJEAB) Vol-1, Issue-4, Nov-Dec- 2016, http://dx.doi.org/10.22161/ijeab/1.4.62 ISSN: 2456-1878.

[7] S. N. Ghate, P. Sapkale and M. Mukhedkar, "Forest Wildfire Detection and Forecasting Utilizing Machine Learning and Image Processing," 2023 International Conference for Advancement in Technology (ICONAT), Goa, India, 2023, pp. 1-8, doi: 10.1109/ICONAT57137.2023.10080840.

[8] M. Rahul, K. Shiva Saketh, A. Sanjeet and N. Srinivas Naik, "Early Detection of Forest Fire using Deep Learning," 2020 IEEE REGION 10 CONFERENCE (TENCON), Osaka, Japan, 2020, pp. 1136-1140, doi: 10.1109/TENCON50793.2020.9293722.

[9] H. Zhang, Z. Zheng and G. Wen, "Wildfire Monitring Based on LSTM and Deep Learning," IGARSS 2022 - 2022 IEEE International Geoscience and Remote Sensing Symposium, Kuala Lumpur, Malaysia, 2022, pp. 2682-2685, doi: 10.1109/IGARSS46834.2022.9883872.

[10] Amirhosein Mosavi, Ataollah Shirzadi, Bahram Choubin, Fereshteh Taromideh, Farzaneh Sajedi Hosseini, Moslem Borji, Himan Shahabi, Aryan Salvati and Adrienn A. Dineva, "Towards an Ensemble Machine Learning Model of Random Subspace Based Functional Tree Classifier for Snow Avalanche Susceptibility Mapping," in IEEE Access, vol. 8, pp. 145968-145983, 2020, doi: 10.1109/ACCESS.2020.3014816.

[11] Bahram Choubin, Moslem Borji, Amir Mosavi, Farzaneh Sajedi-Hosseini, Vijay P. Singh, Shahaboddin Shamshirband, “Snow avalanche hazard prediction using machine learning methods”, Journal of Hydrology, Volume 577, October 2019, 123929, https://doi.org/10.1016/j.jhydrol.2019.123929.

[12] Alexei Pozdnoukhov, Ross S Purves and Mikhail Kanevski, “Applying Machine Learning Methods to Avalanche Forecasting”, Annals of Glaciology 49(1):107-113, 2008, DOI: 10.3189/172756408787814870

[13] B. Bhargava and S. Pasari, "Earthquake Prediction Using Deep Neural Networks," 2022 8th International Conference on Advanced Computing and Communication Systems (ICACCS), Coimbatore, India, 2022, pp. 476-479, doi: 10.1109/ICACCS54159.2022.9785011.

[14] B. Arunadevi, M. M, M. I. Hussain, R. Lakshmi, R. MM and K. Sengupta Das, "Risk Prediction of Earthquakes using Machine Learning," 2022 3rd International Conference on Electronics and Sustainable Communication Systems (ICESC), Coimbatore, India, 2022, pp. 1589-1593, doi: 10.1109/ICESC54411.2022.9885674.

[15] Wang, X.; Zhong, Z.; Yao, Y.; Li, Z.; Zhou, S.; Jiang, C.; Jia, K. Small Earthquakes Can Help Predict Large Earthquakes: A Machine Learning Perspective. Appl. Sci. 2023, 13, 6424. https://doi.org/10.3390/app13116424

[16] Essam Ghamry; Emad K. Mohamed; Mohamed S. Abdalzaher; Mohamed Elwekeil; Dedalo Marchetti; Angelo De Santis, Mostafa Hegy, Akimasa Yoshikawa, Adel Fathy, "Integrating Pre-Earthquake Signatures From Different Precursor Tools," in IEEE Access, vol. 9, pp. 33268-33283, 2021, doi: 10.1109/ACCESS.2021.3060348.

[17] L. Wang, M. Zhang, X. Shen and W. Shi, "Landslide Mapping Using Multilevel-Feature-Enhancement Change Detection Network," in IEEE Journal of Selected Topics in Applied Earth Observations and Remote Sensing, vol. 16, pp. 3599-3610, 2023, doi: 10.1109/JSTARS.2023.3245062.

[18] W. Zhang, Z. Liu, H. Yu, S. Zhou, H. Jiang and Y. Guo, "Comparison of landslide detection based on different deep learning algorithms," 2022 3rd International Conference on Geology, Mapping and Remote Sensing (ICGMRS), Zhoushan, China, 2022, pp. 158-162, doi: 10.1109/ICGMRS55602.2022.9849267.

[19] Silvia Liberata Ullo; Amrita Mohan; Alessandro Sebastianelli; Shaik Ejaz Ahamed; Basant Kumar; Ramji Dwivedi; Ganesh R. Sinha, "A New Mask R-CNN-Based Method for Improved Landslide Detection," in IEEE Journal of Selected Topics in Applied Earth Observations and Remote Sensing, vol. 14, pp. 3799-3810, 2021, doi: 10.1109/JSTARS.2021.3064981.

[20] L. Dwarakanath, A. Kamsin, R. A. Rasheed, A. Anandhan and L. Shuib, "Automated Machine Learning Approaches for Emergency Response and Coordination via Social Media in the Aftermath of a Disaster: A Review," in IEEE Access, vol. 9, pp. 68917-68931, 2021, doi: 10.1109/ACCESS.2021.3074819.